

Acoustic Emission and Ultrasonic Wave Characteristics in TIG-welded 316 Stainless Steel

Jin Kyung Lee^{1,*}, Joon Hyun Lee², Sang Pill Lee¹, In Su Son¹, and Dong Su Bae³

¹Donggeui University, Dept. of Mechanical Engineering, Busan 614-714, Korea

²Pusan National University, School of Mechanical Engineering, Busan 609-735, Korea

³Donggeui University, Dept. of Advanced Materials Engineering, Busan 614-714, Korea

(received date: 22 August 2012 / accepted date: 28 September 2013)

A TIG welded 316 stainless steel materials will have a large impact on the design and the maintenance of in-vessel components including pipes used in a nuclear power plant, and it is important to clear the dynamic behavior in the weld part of stainless steel. Therefore, nondestructive techniques of acoustic emission (AE) and ultrasonic wave were applied to investigate the damage behavior of welded stainless steel. The velocity and attenuation ratio of the ultrasonic wave at each zone were measured, and a 10 MHz sensor was used. We investigated the relationship between dynamic behavior and AE parameters analysis and derived the optimum parameters to evaluate the damage degree of the specimen. By measuring the velocity and the attenuation of an ultrasonic wave propagating each zone of the welded stainless steel, the relation of the ultrasonic wave and metal structure at the base metal, heat affected zone (HAZ) metal and weld metal is also discussed. The generating tendency of cumulated counts is similar to that of the load curve. The attenuation ratios from the ultrasonic test results were 0.2 dB/mm at the base zone, and 0.52 dB/mm and 0.61 dB/mm at the HAZ zone and weld zone, respectively.

Key words: welding, ultrasonics, tensile test, mechanical properties, acoustic emission

1. INTRODUCTION

Stainless steel is the primary candidate as a structural material for the first wall elements and the divertor in a fusion reactor because it has numerous advantages in terms of corrosion resistance and mechanical properties under high temperature. In order to replace the structural components of an international thermonuclear experimental reactor (ITER) [1,2], welding is an effective method for jointing them. Welded materials will have a large impact on the design and the maintenance of in-vessel components including the divertor and first wall elements. Since ITER components jointed by welding are one of many factors limiting the material's lifetime, the conditions of the welded structural components should be monitored while the reactor is working in the field. In this study, the tungsten inert gas welding (TIG) method [3-5] was performed on stainless steel, and a welded specimen of 316 stainless steel was prepared in order to evaluate the microscopic damage behavior on its weld. TIG welding of stainless steel is one of the most common methods used in the industry. An acoustic emission (AE) technique [6-8], one of nondestructive tests for the evaluation of dynamic behavior of materials, was applied

to nondestructively investigate the damage behavior of the welded specimen. AE technique is a method to analyze the elastic waves caused by dislocation, cracks initiation, and propagation within material from external loads. There are many parameters such as energy, duration time, event, and amplitude in order to analyze the dynamic behavior of the specimen in AE technique. We investigated the relationship between dynamic behavior and AE parameters analysis and derived the optimum parameters to evaluate the damage degree of the specimen. However, an ultrasonic test (UT) [9-11] is a useful method to evaluate the mechanical properties of material. By measuring the velocity and the attenuation of the ultrasonic waves propagating each zone of the welded stainless steel, the relation of ultrasonic wave and metal structure at the base metal, heat affected zone (HAZ) metal, and weld metal was also discussed. Ultrasonic waves were also used to evaluate the defects in the welded stainless steel pipe, and the amplitude of the wave according to the defects size was studied.

2. EXPERIMENTAL PROCEDURES

Figure 1(a) shows the experimental procedure to examine the damage behavior using the AE system and the tensile strength of the welded specimen. As shown in Fig. 1(a), an

*Corresponding author: leejink@deu.ac.kr
©KIM and Springer

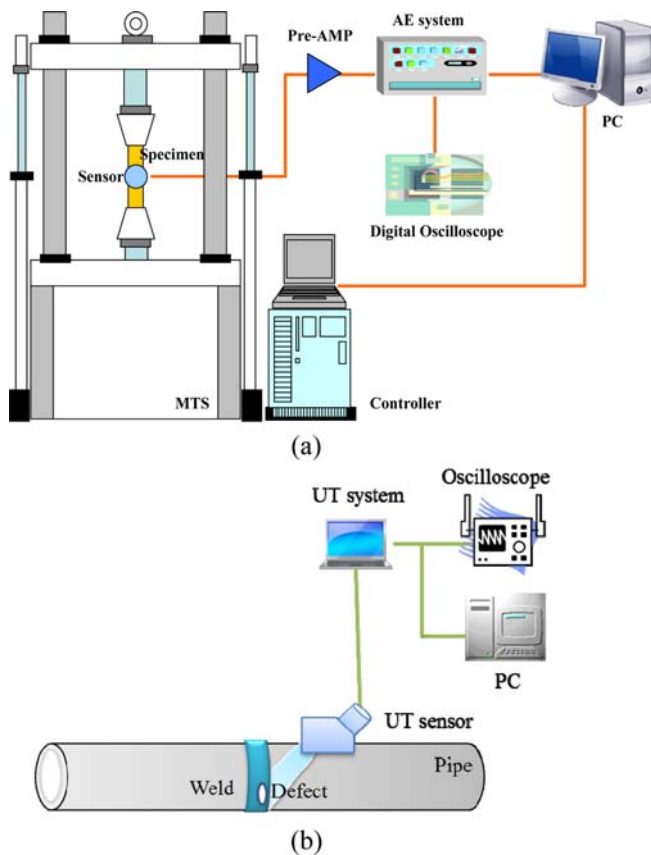


Fig. 1. Schematic diagram of experimental set up to evaluate the characteristics of welded STS 316 specimen using AE technique (a), and to evaluate the defects using ultrasonic waves (b).

AE sensor is attached at the middle of the 316 stainless steel specimen, and load is applied to the specimen at 12 mm/min. The specimen emits numerous elastic waves caused by dislocations, deformation, and cracks due to external loadings, and the AE sensor receives these elastic waves. The signals at the sensor are so weak that the AE system cannot analyze their characteristics. Therefore, the received signals at the AE sensor are amplified by 40dB at the pre-AMP. The amplified signals at the pre-AMP are analyzed at the main AE system by AE parameters such as amplitude, energy, duration time, and frequency. Each parameter shows various values according to the degree of damage by external loading. The optimal parameter for nondestructively measuring the damage of the 316 stainless steel can be found by comparing the change of AE parameters with the damage degree of the specimen. One of the main objectives of the present study is to find optimal parameters showing a close relationship between the AE parameters and damage. The used sensor is wideband (100-1200 kHz), and the threshold level for eliminating electrical and mechanical noises is fixed to 40dB. In addition, in order to evaluate the characteristics of metal structure according to base metal, welding metal and HAZ metal ultrasonic technique was applied. The ultrasonic test was performed by immer-

sion technique in which the specimen was submerged in water to eliminate the influence of couplant. The velocity and attenuation ratio of ultrasonic waves at each zone were measured, and a 10 MHz sensor was used. The surface morphology of the welded specimen at each zone was also observed with a microscope. However, Fig. 1(b) shows the schematic of ultrasonic wave (UT) system to evaluate the defects in the welded pipe. The artificial defects of 3 mm, 5 mm, 10 mm, 15 mm, and 20 mm were induced in the weld region, and a 60 wedge and a 2.25 MHz sensor were used to detect the defects. The amplitude of ultrasonic waves reflecting from the defects was analyzed at the digital oscilloscope (LeCroy). The wall thickness of the welded stainless steel was 10 mm.

3. RESULTS AND DISCUSSION

3.1. Mechanical properties and AE characteristics for the welding zone of the 316 stainless steel

Figure 2 shows the characteristics of AE parameters for the TIG-welded STS 316 specimen as load increases. As shown in Fig. 2(a), remarkable number of AE events were generated at the beginning of the load, and the number of events gradually decreased after the yielding point. The AE event did not show a considerable increase at the stage of severe plastic behavior of the specimen. A large number of AE events occurred due to the appearance of large cracks when the specimen was completely broken. Cumulated AE counts showed a rapid increase at the first stage of loading and gradually increased through plastic zone. As shown in Fig. 2(b), the generating tendency of cumulated counts is similar to the load curve. Therefore, it is found that cumulated counts curve can estimate the mechanical properties, including the yield point, tensile strength, and elastic modulus, of TIG-welded SUS 316 material. The remarkable increase of AE events and cumulated counts until the yield point is caused by the unstable conditions within the weld material, the micro deformation at beginning of load, and noise from grips of the tensile tester holding the specimen. Figures 2(c) and (d) represents the amplitude and the average frequency of the generated AE signals. The signals usually showed a range between 40dB and 65dB in amplitude from the specimen under all range of load including elastic and plastic zones, but many AE signals were above 65dB in amplitude at the load under yield point. These signals are due to the deformations of the weld metal and HAZ metal, as well as discontinuous matters of small porosities and tungsten inclusions within weld metal in the microscope observation. Such high signals in amplitude did not appear in the AE test of the pure STS 316 material. The average frequency of Fig. 2(d) represents that the range of average frequency for most AE signals is below 300 kHz. Several signals above 400 kHz appear near the yielding points. From these results it was found that AE signals from weld metal and HAZ metal are higher than those of base metal in

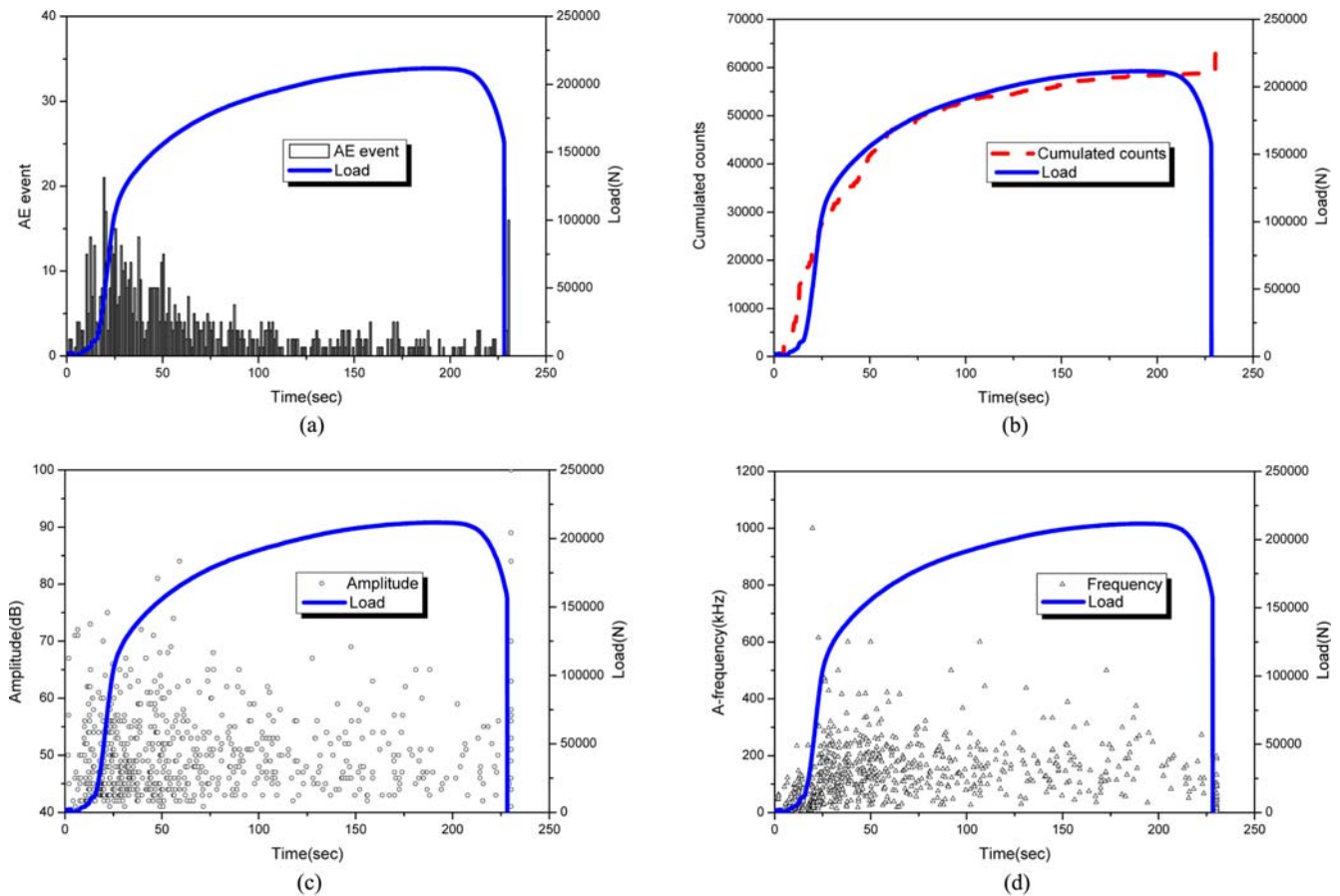


Fig. 2. AE parameters according to the load increase: (a) AE event, (b) Cumulated count, (c) Amplitude and (d) Average frequency

amplitude and average frequency among AE parameters.

Figure 3 shows the typical waveforms and frequency characteristics of the AE signal generated at each stage of load. As shown in Fig. 3, all waveforms at each stage of load are burst type, but their amplitudes differ according to the stages of load. At the first stage of load, the amplitude of the waves is a little higher than those of signals generated during the middle stage (entire plastic zone), while the amplitude of signals at the end of load are remarkably high. This signal is from the appearance of a macro-crack by complete fracturing of the specimen. The main frequency range of the signal at the beginning of load is 427 kHz, and the signal shows a frequency component of around 970 kHz. However, the frequency component of 935 kHz and 970 kHz is the main frequency range in the middle and at the end of the load. Signals above 900 kHz in frequency did not appear in the test of base metal. Therefore, the signals in the middle and at the end of the load are believed to be affected by the TIG welding, and this can be explained from fact that a macro-crack appeared at the boundary of base metal and HAZ metal when the specimen was completely broken. Compared to base metal, the welded specimen did not show a big difference in waveform but was much higher in the frequency spectrum.

3.2. Ultrasonic wave characteristics for the welding zone of 316 stainless steel

Figure 4 is a photograph of each zone of the 316 stainless steel specimen. The surface of the specimen was polished with sand paper (#1500) and diamond power (10 nm) to measure the velocity and the attenuation ratio of an ultrasonic wave. The velocity and the attenuation ratio was measured at three points of the each metal zone, and we took an average of them. The thickness of the specimen was 3.5 mm, and the frequency of UT sensor was 10 MHz. In addition, the Vickers hardness (Mitutoyo Corp., 0.1 kgf-980.7 mN) and Rockwell hardness (Kyungdo Corp., 100 kg-ball) were measured in each metal and are shown in Table 1. Table 2 shows the chemical composition of each metal, and the change of composition in each metal makes the difference in the hardness and parameters of ultrasonic waves.

The metals can be ranked from hardest to softest as follows: weld metal, HAZ metal, and base metal. These changes in hardness according to each metal are due to structure changes in the metal due to welding, such as the appearance of chromium carbide. The changes in metal structure are shown in Fig. 4. However, the typical waveform of ultrasonic waves propagating throughout the specimen is shown in Fig. 5. As shown

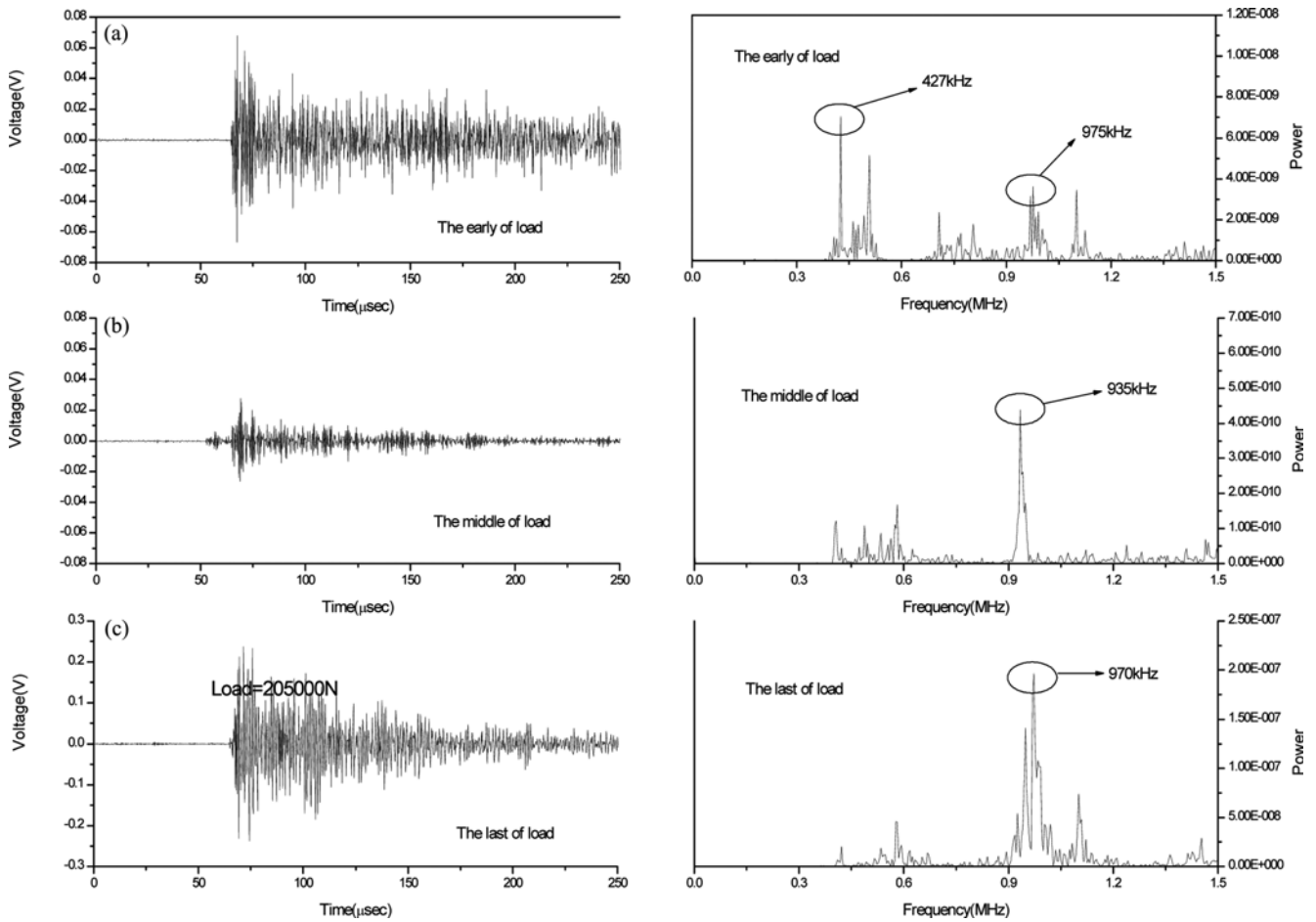


Fig. 3. The typical waveforms and frequency spectrum at each stage of load: (a) 25000N, (b) 180000N and (c) 205000N.

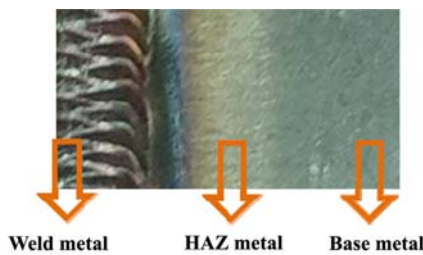


Fig. 4. Photograph of each zone of the specimen.

Table 1. Hardness according to each metal

Hardness	Metal		
	Base metal	HAZ metal	Weld metal
Vickers(Hv)	184.6	192.9	204.8
Rockwell(HRB)	84.9	89.8	96.8

in Fig. 5, the amplitude of the waveform was the highest at the base metal and lowest at the weld metal. The velocity was calculated by measuring the time difference (Δt) of the two waves and the specimen thickness. The attenuation ratio was also computed by the amplitude of reflected waves. Figure 6

Table 2. Chemical composition of each metal (wt%)

Metal	Composition				
	Fe	Cr	Ni	C	O
Base metal	54.8	17.35	8.08	7.98	11.78
HAZ metal	39.01	17.41		20.09	20.58
Weld metal	63.98	17.08		15.09	2.02

shows the velocity and attenuation of ultrasonic waves according to each place of the welded specimen. As shown in Fig. 6 the velocity is 5723 m/s at the base metal, 5768 m/s at the HAZ metal, and 5672 m/s at the weld metal. The difference in velocity at each metal is within 1%, and it is within a very small range of the experimental error. Therefore, the velocities are almost identical according to each zone of the welded specimen. However, attenuation ratios are 0.2 dB/mm at base metal, and 0.52 dB/mm and 0.61 dB/mm at HAZ metal and weld metal, respectively. The attenuation ratio linearly increased with base metal, HAZ metal, and weld metal, in that order. The attenuation of ultrasonic waves represented a significant difference in each metal. This is related to the metal structure. As shown in Fig. 6, many large and small inclusions and

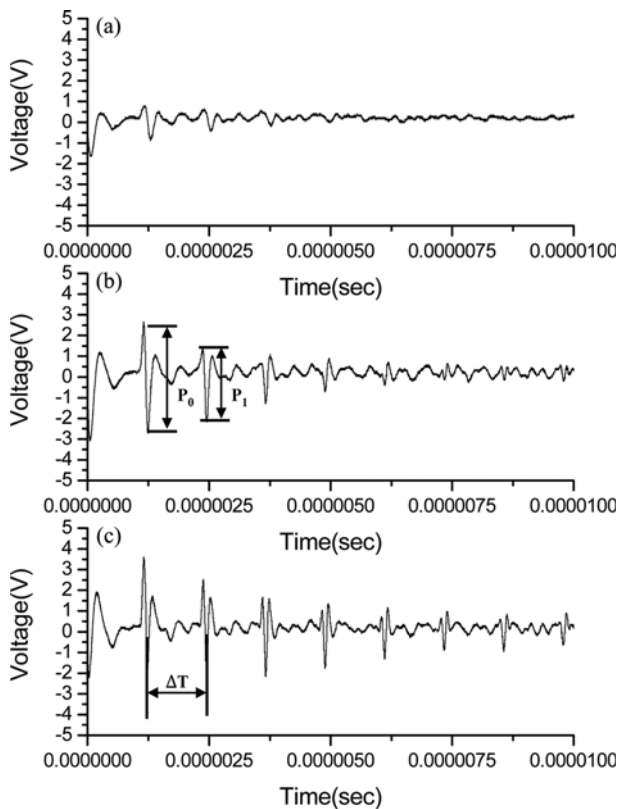


Fig. 5. Typical waveforms of ultrasonic waves at each zone of the specimen: (a) Weld metal, (b) HAZ metal and (c) Base metal.

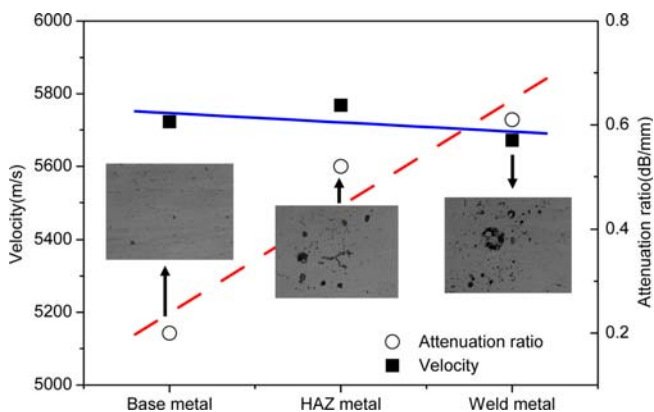


Fig. 6. The velocities and the attenuation ratios of ultrasonic waves at each zones of the specimen.

chromium carbides have been found within the HAZ metal and weld metal. These chromium carbide particles and containments give a large influence at the propagation of ultrasonic waves and scatter the ultrasonic wave. The attenuation ratio is also higher at this zone of the specimen than at the base metal.

Figure 7 shows the result of an ultrasonic wave reflecting from the defects according to the defect sizes in the welded pipe. As shown in Fig. 7, the amplitudes of the reflected ultrasonic

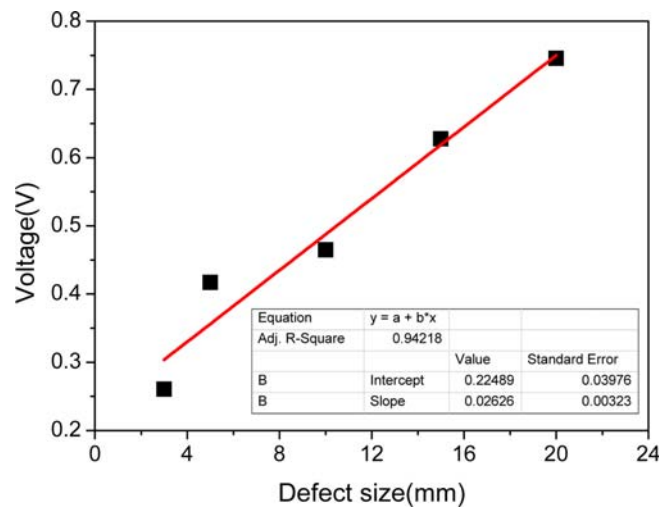


Fig. 7. Amplitude of an ultrasonic wave reflecting from the defects according to the defect sizes.

wave in the specimen with a defect of 3 mm were around 0.25 V and 0.75 V in the specimen with a defect of 20 mm. The amplitudes were linearly increased as the size of the defect increased. In general, the energy of the reflected ultrasonic wave from the defect increases by increasing the size of the defect. Therefore, the energy of the reflected ultrasonic from the specimen having a 20 mm defect was considerably higher than that of specimen having a 3 mm defect, and this tendency shows a linear increase with defect sizes. Therefore, it is found that the defects size in the welded stainless steel pipe can be estimated by measuring the amplitude of ultrasonic waves.

4. CONCLUSIONS

From study on nondestructive technique using the acoustic emission and ultrasonic waves to evaluate the damage and mechanical properties of welded SUS 316 stainless steel, the following conclusions were drawn.

(1) A remarkable number of AE events are generated at the beginning of the load, and the number of events gradually decreased after yielding point.

(2) The generating tendency of cumulated counts is similar to the load curve. Therefore, we could estimate the mechanical properties including the yielding point, tensile strength, and elastic modulus of TIG-welded SUS 316 material from cumulated counts curve.

(3) All waveforms at each stage of load are burst type, but their amplitudes differ according to the stages of load. The main frequency range of the signal at the beginning of the load is 427 kHz, and 935 kHz and 970 kHz in the middle and the end of load, respectively.

(4) The velocities are almost identical according to each zone of the welded specimen. The attenuation ratios are

0.2 dB/mm at base metal, and 0.52 dB/mm and 0.61 dB/mm at HAZ metal and weld metal, respectively.

(5) Using ultrasonic waves was an useful method to evaluate the defects in the weld region because the amplitude reflecting from the defect in the welded pipe linearly increased as the defects size increased.

ACKNOWLEDGMENTS

This work was supported by Korea Institute of Energy Technology Evaluation and Planning (KETEP), through its Technology Innovation Program of Nuclear Power Plants.

REFERENCES

1. H. W. Bartels, *Fusion Engineering and Design* **51-52**, 401 (2000).
2. J. K. Lee, S. P. Lee, and J. H. Byun, *Fusion Engineering and Design* **85**, 1376 (2010).
3. G. Lothongkum, E. Viyanit, and P. Bhandhubanyong, *J. of Materials Processing Tech.* **110**, 233 (2001).
4. K. Tsuchiya, H. Kawamura, and G. Kalinin, *J. of Nuclear Mater.* **283**, 1210 (2000).
5. S. C. Juang and Y. S. Tarn, *J. of Materials Processing Tech.* **122-1**, 33 (2002).
6. M. Fregonese, H. Idrissi, H. Mazille, L. Renaud, and Y. Cetre, *J. of Mater. Science* **36**, 557 (2001).
7. J. C. Jeong, D. J. Yoon, P. L. Park, K. B. Kim, and S. S. Lee, *J. Kor. Inst. Met. & Mater.* **40**, 853 (2002).
8. I. Read, P. Foote, and S. Murray, *Measurement Science & Technology* **13-1**, 5 (2002).
9. K. C. Kim, H. Fukuhara, and H. Yamawaki, *Japanese Journal of Applied Physics Part 1-Regular Papers Short Notes & Review Papers* **41-1**, 374 (2002).
10. R. Demirli and J. Saniie, *IEEE Transactions on Ultrasonics Ferroelectrics & Frequency Control* **48-3**, 787 (2001).
11. A. J. Moysan, G. Corneloup, T. Fouquet, and B. Chassignole, *Ultrasonics* **43**, 447 (2005).